



1 Development and Assessment of a High Spatial Resolution 2 (4.4 km) MISR Aerosol Product Using AERONET-DRAGON 3 Data

4
5 **M. J. Garay¹, O. V. Kalashnikova¹, and M. A. Bull¹**

6 [1]{Jet Propulsion Laboratory, California Institute of Technology, Pasadena, California}

7 Correspondence to: M. J. Garay (Michael.J.Garay@jpl.nasa.gov)

8

9 Abstract

10 Since early 2000, the Multi-angle Imaging SpectroRadiometer (MISR) instrument on
11 NASA's Terra satellite has been acquiring data that has been used to produce aerosol optical
12 depth (AOD) and particle property retrievals at 17.6 km spatial resolution. Capitalizing on
13 the capabilities provided by multiangle viewing, the current operational (Version 22) MISR
14 algorithm performs well with about 75% of MISR AOD retrievals globally falling within 0.05
15 or 20% \times AOD of paired validation data from the ground-based Aerosol Robotic Network
16 (AERONET). This paper describes the development and assessment of a prototype version of
17 a higher spatial resolution, 4.4 km MISR aerosol product compared against multiple
18 AERONET Distributed Regional Aerosol Gridded Observations Network (DRAGON)
19 deployments around the globe. We find that, overall, the 4.4 km AOD retrievals perform
20 much better than the 17.6 km retrievals in comparison to the AERONET-DRAGON data for
21 over 100 individual sites. In particular, the previously reported underestimation of AOD at
22 high AOD in the operational 17.6 km product appears to be largely eliminated.

23

24 1 Introduction

25 Atmospheric aerosols, suspended particles of solid and liquid, play key roles in the weather
26 and climate of the Earth. Aerosol optical depth (AOD) is a fundamental parameter that
27 expresses the amount of aerosol in the atmospheric column and its effect on the transmission
28 of sunlight. Global observations of aerosol amount depend fundamentally on retrievals of



1 AOD from instruments on satellite platforms, such as Multi-angle Imaging
2 SpectroRadiometer (MISR) and the MODerate resolution Imaging Spectroradiometer
3 (MODIS) that fly on the NASA Earth Observing System (EOS) Terra satellite. Satellite
4 aerosol observations are used to model the global radiation budget and investigate the effects
5 of aerosols on clouds (e.g., Boucher et al., 2013). Applications of satellite-derived AOD
6 information include air quality and health studies that use satellite-retrieved AOD to estimate
7 ground-level concentrations of particulate matter, especially particles with aerodynamic
8 diameter less than $2.5\text{ }\mu\text{m}$ ($\text{PM}_{2.5}$), which are known to have significant health effects due to
9 their ability to penetrate the human respiratory system (e.g., Martin, 2008; van Donkelaar et
10 al., 2015; 2016).

11 Critical to the success of satellite aerosol missions like MISR and MODIS are assessments of
12 the performance of their retrieval algorithms. Algorithm performance is typically evaluated
13 by the ability of the retrievals to capture the observed spatiotemporal variability of aerosols as
14 determined by ground-based observations, which are taken to represent the “truth.” Within
15 the satellite aerosol community, the Aerosol Robotic Network (AERONET) is often used as a
16 standard, global reference. AERONET is a federated instrument network of ground-based
17 sunphotometers that derive AOD at a number of visible and near-infrared wavelengths from
18 direct sun observations (Holben et al., 1998).

19 The MISR instrument has been acquiring data from on board the NASA Terra Earth
20 Observing System (EOS) platform since early 2000. The current Level 2 (swath-based)
21 aerosol retrieval algorithm, designated F12_0022, or Version 22 (V22), began production at
22 the NASA Langley Research Center Atmospheric Science Data Center (ASDC) on 1
23 December 2007, and has been applied to the entire MISR mission, including current (forward)
24 processing. Details of the V22 MISR aerosol retrieval over water and land can be found in
25 Kalashnikova et al. (2013) and Martonchik et al. (2009), respectively. AOD and associated
26 aerosol particle properties are reported in the MISR aerosol product on a 17.6 km spatial
27 resolution grid, which represents 16×16 (256) samples of the 1.1 km resolution MISR
28 observations in four spectral bands in the visible and near infrared made from nine separate
29 viewing angles (Diner et al., 1998). The MISR aerosol product was evaluated against global
30 AERONET sites by Kahn et al. (2010), who reported that, overall, about 70% to 75% of
31 MISR AOD retrievals are within the greater of 0.05 or $0.2 \times \text{AOD}$ of the paired AERONET
32 data. By way of comparison, the operational MODIS Collection 6 (C6) Dark Target (DT)



1 algorithm, which began production in 2014, has a reported expected error (EE) envelope,
2 containing about 67% of the retrievals relative to AERONET, of $-(0.02 + 0.1 \times \text{AOD})$ to
3 $+(0.04 + 0.1 \times \text{AOD})$ (Levy et al., 2013). Sayer et al. (2015) found that about 85% of
4 vegetated sites and 70% of arid sites fell within the EE envelope of $\pm(0.05 + 0.2 \times \text{AOD})$ for
5 the MODIS C6 Deep Blue (DB) algorithm for MODIS-Terra after the application of
6 calibration corrections for the sensor.

7 Kahn et al. (2010) also identified a number of issues in the performance of the V22 MISR
8 aerosol retrieval algorithm, including a small gap at low AODs relative to AERONET and the
9 appearance of quantization noise, missing particles in the aerosol look up table, and a frequent
10 underestimate of AOD relative to AERONET over land when the AOD was greater than
11 about 0.4. Subsequently, Kalashnikova et al. (2013), Witek et al. (2013), and Shi et al. (2014)
12 identified issues with the cloud screening applied in the V22 algorithm, especially with regard
13 to thin cirrus, and suggested possible solutions; and Limbacher and Kahn (2015) diagnosed
14 the effects of stray light in the MISR cameras, noted earlier by Bruegge et al. (2002), that
15 could have significant impact on retrieved AODs in scenes with high contrast. These efforts
16 by members of the MISR science team and others have been directed at improving the quality
17 of the MISR aerosol product with the view of delivering a new version of the operational
18 MISR aerosol retrieval algorithm in the near future. At the same time, a number of studies
19 have highlighted the need for aerosol products at higher spatial resolutions than currently
20 available operationally from MISR and MODIS, gridded at 17.6 km and 10.0 km,
21 respectively. In response to this, the MODIS team released a global 3 km resolution DT
22 aerosol product as part of its Collection 6 delivery (Remer et al., 2013). In this work, we
23 describe the effort to develop a higher resolution, 4.4 km Level 2 MISR aerosol product based
24 on initial tests that showed significant retrieval improvement relative to AERONET sites
25 deployed in relatively large numbers in Distributed Regional Aerosol Gridded Observations
26 Network (DRAGON) campaigns around the globe (e.g., Eck et al., 2014; Seo et al., 2015;
27 Sano et al., 2016). In the DRAGON networks, instruments are located much closer to one
28 another, with a typical grid spacing around 10 km (e.g., Munchak et al., 2013). As we will
29 discuss in this paper, we found that the new MISR 4.4 aerosol product is better able to resolve
30 spatial gradients in AOD compared to the operational (V22) 17.6 km resolution product as
31 shown in a number of comparisons from different DRAGON deployments that encompass a
32 wide range of aerosol loadings.



1

2 **2 Data and methods**

3 **2.1 20 January 2013 MISR overpass of DRAGON San Joaquin Valley,** 4 **California**

5 The initial motivation for this work was a MISR overpass of the DRAGON sites deployed in
6 the San Joaquin Valley of California in support of the NASA Deriving Information on
7 Surface conditions from Column and Vertically Resolved Observations Relevant to Air
8 Quality (DISCOVER-AQ) field campaign in January and February 2013 (see Beyersdorf et
9 al., 2016). Figure 1a shows the red band (672 nm) image from MISR Orbit 69644 when the
10 Terra satellite passed over the San Joaquin Valley around 18:50 UTC on 20 January 2013.
11 The image is oriented with north to the top. The bright features in the upper central portion of
12 the image are snow in the Sierra Nevada, with the San Joaquin Valley of central California to
13 the southwest. Figure 1b shows the green band (558 nm) AOD reported in the MISR V22
14 operational aerosol product at 17.6 km resolution. The circles correspond to the AODs
15 reported by the AERONET-DRAGON sites closest in time to the Terra overpass using the
16 same color scale as the MISR AODs. The horizontal lines denote the MISR “blocks” that
17 correspond to 141 km in the along-track direction of the satellite motion (Bothwell et al.,
18 2002). It is clear in Fig. 1b that the aerosols are concentrated in the San Joaquin Valley,
19 although on this date the AOD is relatively low, with a maximum around 0.30.

20 As mentioned above, the V22 MISR aerosol retrieval algorithm takes as input the 256 – 1.1
21 km MISR Level 1B2 pixels within the 17.6 km retrieval region (16 pixels × 16 pixels). In
22 standard “global” acquisition mode, blue, green, and near infrared bands in the off-nadir
23 cameras are averaged onboard from the full 275 m pixel resolution to 1.1 km to save data rate,
24 while the red bands in all nine cameras and the blue, green, and near infrared bands for the
25 nadir camera are preserved at their full resolution (Diner et al., 1998). The 1.1 km pixel data
26 for the red band and the nadir camera are calculated by the aerosol algorithm by simple
27 averaging. The MISR instrument has another “local” acquisition mode that preserves the full
28 resolution of the data for all nine cameras and four spectral bands for a target with an along-
29 track length of about 300 km (Diner et al., 1998). It was recognized that with some
30 modifications the V22 algorithm could be applied to this “local mode” data, resulting in a
31 product with 4.4 km spatial resolution due to the change of the input resolution from 1.1 km



1 to 275 m (since $275 \text{ m} \times 16 = 4.4 \text{ km}$). Figure 1c shows the results of the application of the
2 modified V22 algorithm to a local mode acquisition made over Pixley, CA (PIXLEYCA),
3 which accounts for the smaller geographic coverage of the retrieval. The same color scale is
4 applied to the AOD retrievals in this case as in Fig. 1b, and, again, the AERONET-DRAGON
5 sites are indicated by circles colored by the AOD reported for the time nearest the Terra
6 overpass. Not only is much greater detail revealed regarding the spatial distribution of
7 aerosols in the San Joaquin Valley, with higher aerosol loading extending from the Fresno in
8 the central part of the valley to Bakersfield in the southeast, but visually the agreement
9 between the MISR AODs and the AERONET-DRAGON AODs is much improved.

10 The visual impression of better agreement is borne out in the regression analysis shown in
11 Fig. 2. Figure 2a compares the 17.6 km V22 AODs from MISR at 558 nm with the
12 AERONET AODs linearly interpolated from the two nearest wavelengths on either side in
13 log-log space to 558 nm (e.g., Sayer et al., 2013). The matches are made nearest in time to
14 the Terra overpass (typically within 15 minutes) and the AERONET observations are required
15 to fall within a specific 17.6 km retrieval region. These criteria are somewhat different than
16 the matching criteria used in Kahn et al. (2010), who considered the average AOD of
17 AERONET observations within a 2 h window centered at the time of the satellite overpass,
18 with at least one valid observation within the hour before and one in the hour after. They also
19 considered MISR retrievals in both the “central” 17.6 km region and the eight surrounding
20 regions. The interpolation of the AERONET AODs to the MISR wavelength was also done
21 slightly differently by Kahn et al. (2010), who used a second order polynomial fit, but this
22 resulted in a negligible change in the results for this particular case. As in Kahn et al. (2010)
23 the analysis here uses the “best-estimate” MISR AODs, which correspond to the mean of the
24 AODs for all the mixtures in the MISR look up table that pass the acceptance criteria. For the
25 17.6 km MISR retrieval there are 11 temporal and spatial matches with the AERONET data.
26 The correlation coefficient, r , is 0.6563; the root mean squared error (RMSE) is 0.0499; the
27 bias is -0.0233 ; and the percent of data within the EE envelope of MISR (the greater of 0.05
28 or $0.20 \times \text{AOD}$) is 72.73%. These results show the 17.6 km V22 retrieval performs relative to
29 the AERONET-DRAGON observations in a way that is generally consistent with the global
30 performance of the algorithm as assessed by Kahn et al. (2010).

31 Figure 2b shows the regression of the 4.4 km MISR aerosol retrieval using the slightly
32 modified V22 algorithm and the 275 m local mode input. Now, the correlation coefficient is



1 0.9144, the RMSE is 0.0184, the bias is -0.0060 , and 100% of the data fall within the EE
2 envelope. These are all significant improvements in the agreement between the MISR aerosol
3 retrieval and the AERONET-DRAGON observations. The sampling was reduced by two
4 points, but inspection of the results shows that the data points that were eliminated due to the
5 requirement that the AERONET site fall within the 4.4 km retrieval region were both already
6 in good agreement with the 17.6 km MISR aerosol retrieval, which means that the
7 improvement is not simply due to the exclusion of outliers in the comparison. Over years of
8 refinements applied to the 17.6 km retrieval to improve performance relative to AERONET,
9 the results in Fig. 2 are among the most significant that were ever obtained. Note that these
10 results are also in contrast to the results of Remer et al. (2013) regarding the MODIS 3 km DT
11 retrievals. They reported that agreement of the 3 km retrieval relative to AERONET was
12 slightly worse over land compared to the 10 km retrieval, while the performance was similar
13 over ocean. The EE envelopes were found to be $\pm 0.05 \pm 0.20 \times \text{AOD}$ and $\pm 0.03 \pm 0.05 \times \text{AOD}$
14 for land and ocean, respectively.

15 A further point is that the unique, high density nature of the AERONET-DRAGON
16 deployment is important for assessing the ability of a high resolution aerosol retrieval
17 algorithm to capture the true spatial variability of aerosols within a region. As shown in Fig.
18 1, the higher resolution MISR aerosol retrieval is better able to represent the spatial gradients
19 in the aerosol load, even though the aerosol load is relatively low on this date and aerosols are
20 spread throughout the San Joaquin Valley. In this case, both the 17.6 km and 4.4 km
21 retrievals report nearly identical values for the Fresno_2 site AERONET site, which is the
22 “permanent” site in the San Joaquin Valley and not part of the DRAGON deployment. So
23 comparisons with this single site would not reveal any important difference in the two
24 versions of the algorithm. Of course, a single case cannot support the conclusion that the 4.4
25 km MISR retrieval is superior to the 17.6 km retrieval in an overall sense, so further
26 comparisons were made with AERONET-DRAGON deployments around the globe in a
27 variety of aerosol loading situations. Even so, the results from the 20 January 2013 case were
28 sufficiently encouraging to focus the MISR science team on the development of a 4.4 km
29 spatial resolution retrieval that would not rely on local mode data to achieve the resolution
30 improvement, but would work with the 1.1 km global mode data.



2.2 AERONET-DRAGON deployments

According to the AERONET website (http://aeronet.gsfc.nasa.gov/new_web/dragon.html), there have been nine AERONET-DRAGON deployments between 2011 and 2016. However, the 20 January 2013 MISR case was instructive in terms of specific characteristics of a deployment necessary to facilitate a comparison of the 17.6 km resolution aerosol retrieval with a higher resolution 4.4 km retrieval. The primary consideration involves the number and density of sites in the deployment. Table 1 shows an evaluation of eight of the nine DRAGON deployments in terms of the spatial statistics. The on-going deployment of DRAGON as part of the KORUS-AQ field campaign in South Korea, Japan, and China was not considered here.

Starting with the San Joaquin Valley deployment, the table shows that 28 sites were deployed. This results in 378 pairs (28 choose 2). Calculating the separation between each pair, there are seven pairs separated by less than 17.6 km, 3 pairs separated by less than 8.8 km, and 1 pair separated by less than 4.4 km. The mean distance between pairs is 245.7, while the median distance is 204.8 km. The MISR analysis is facilitated by a relatively large number of pairs separated by less than 17.6 km that can be used to test the ability of the 4.4 km algorithm to retrieve spatial gradients, but few pairs separated by less than 4.4 km, which will likely fall inside a single 4.4 km retrieval region. The swath and orbit characteristics of MISR must also be taken into account. MISR has a swath of about 400 km and Terra has a repeat cycle of 16 days. Deployments with widely separated clusters of sites will therefore only provide a limited number of comparisons for a particular MISR overpass. Cloudiness is a further consideration as the DRAGON deployments typically happen within a limited time frame – about a month in the case of San Joaquin Valley.

Based on these considerations, and visual inspections of candidate scenes, a set of MISR cases was identified during DRAGON deployments for testing the 4.4 km and 17.6 km resolution aerosol retrievals relative to AERONET. This set is shown in Table 2. In the table, the “SOM Path” corresponds to the Space-Oblique Mercator (SOM) projection onto the World Geodetic System 1984 (WGS84) ellipsoid used for the MISR processing (Diner et al., 1998). There are 233 SOM paths within each 16-day repeat cycle of Terra. The cases are broadly classified in terms of the range of AODs, with “low AOD” representing AODs generally less than 0.3, “moderate AOD” corresponding to AODs between about 0.3 and 0.6, and “high AOD” having AODs between about 0.6 and 1.4. Note that while the cases are



distributed globally including Washington D.C./Baltimore; the San Joaquin Valley in California; Seoul, South Korea; and Osaka, Japan; a limitation of this study is that the AERONET-DRAGON deployments have been primarily to mid-latitude locations, so there are no cases from tropical, arid desert, or polar regions.

Figure 3 provides maps of the four relevant AERONET-DRAGON deployments. Figure 3a shows the locations of 45 of the 46 sites deployed in 2011 for the Washington, D.C./Baltimore campaign. The sites are generally located around the greater Baltimore area. For reference, the distance between Washington, D.C. and Baltimore, MD is about 56 km. Also, recall that 1 degree of latitude corresponds to about 111 km, which provides another reference. Figure 3b shows the 25 sites deployed in South Korea in 2012. The majority of sites are clustered around Seoul with a relatively large number of sites spaced less than 4.4 km apart, as shown in Table 1. Even so, the overall number of sites makes this a reasonable test case for the 4.4 km MISR algorithm. Additionally, the cases from South Korea offer situations with high AOD. Figure 3c shows the 18 AERONET-DRAGON sites deployed in the San Joaquin Valley of California. Compared to the other cases, the density of sites in this deployment is somewhat less, but this provides good sampling of the aerosol distribution throughout the valley. Finally, Fig. 3d shows the locations of the 14 AERONET-DRAGON sites deployed around Osaka, Japan in 2012. The largest density of sites is around Osaka, itself. Again, the spatial clustering of sites is less than ideal, since many of them are separated by less than 4.4 km.

2.3 MISR aerosol retrievals over land

Details of the MISR aerosol retrieval over land, which is most relevant to comparisons with AERONET-DRAGON, can be found in Martonchik et al. (2009). The fundamental principal of the retrieval is the separation of the multi-angular satellite signal at the top of the atmosphere (TOA) into a component due to the aerosols and a component due to multiple surface-atmosphere interactions. The primary underlying physical assumptions are the following:

1. Aerosols are horizontally homogeneous in the retrieval region.
2. A predefined set of aerosols stored in a look up table is applied globally to retrievals over both land and water.



- 1 3. One or more cost functions (χ^2 parameters) are assessed to determine how well
- 2 modelled TOA radiances from individual aerosol models and associated green-band
- 3 AODs match the observed TOA radiances.
- 4 4. The angular shape of the surface reflectance is assumed to be spectrally invariant and
- 5 this is used to filter out models and AODs that do not conform to this assumption as
- 6 being unlikely candidates for selection (Diner et al., 2005).
- 7 5. There is sufficient surface contrast in the retrieval region so that the TOA radiances
- 8 can be represented by empirical orthogonal functions (EOFs) generated directly from
- 9 the multiangle imagery.
- 10 6. No retrievals are performed over complex terrain.
- 11 The choice of acceptable 1.1 km subregions within the retrieval region is done through the
- 12 application of a number of tests including cloud masking.

13

14 **3 Results**

15 **3.1 Regression analysis**

16 Figure 4a shows the regression of the V22 17.6 km MISR green-band AODs against the
17 AERONET-DRAGON AODs interpolated to the MISR wavelength for all the cases listed in
18 Table 2. The range of AODs in this figure is much greater than the AOD range in Fig. 2.
19 Like the regressions shown in Kahn et al. (2010) the underestimation of the retrieved AODs
20 relative to AERONET for AODs greater than about 0.4 is apparent in this figure. By way of
21 comparison, Fig. 4b shows the regression for a prototype 4.4 km MISR aerosol retrieval
22 (internally designated V22b24-34+1) that takes the 1.1 km spatial resolution global mode data
23 as input. Tests showed that the retrieval algorithm did not perform significantly differently
24 when using 275 m local mode data as input compared to the 1.1 km global mode data.

25 The primary difference apparent in Fig. 4 is the improved performance of the 4.4 km
26 algorithm at high AODs. The fall-off evident in the V22 17.6 km resolution retrievals is
27 greatly mitigated, if not eliminated entirely, but it is difficult to tell if any residual bias exists
28 at large AODs due to the small sample size in this AOD range. Comparing the statistics, the
29 sampling is much greater for the 4.4 km resolution retrieval. This is primarily due to the
30 relaxation of the thresholds on the χ^2 parameters to admit better spatial coverage in the 4.4 km



1 retrieval. The need for this change was apparent when looking at maps constructed from the
2 4.4 km retrievals using the initial thresholds. The other parameters all show significant
3 improvements as well. The correlation coefficient goes from 0.8772 to 0.9595; the RMSE
4 decreases from 0.1683 to 0.0768; the bias decreases, in an absolute sense, from -0.0887 to $-$
5 0.0208 , driven primarily by the improvement in the performance of the algorithm at large
6 AODs; and the percent of data within the MISR EE envelope increases from 59.09% to
7 80.92%. Although the statistics from this sample are insufficient for a complete analysis, the
8 last result suggests that the performance of the 4.4 km resolution algorithm will permit the
9 setting of a somewhat tighter EE envelope.

10 **3.2 Example images**

11 Besides providing improved regressions in AOD when compared with observations from the
12 AERONET-DRAGON sites, the greatest benefit of the 4.4 km resolution MISR aerosol
13 retrievals is most apparent when comparing maps of the retrieved AOD with the operational
14 V22 17.6 km algorithm. Figure 5 shows the MISR AOD retrievals for Orbit 65731 over
15 Osaka, Japan on 27 April 2012 at about 01:55 UTC. As shown in the MISR red band image
16 in Fig. 5a, the scene is extremely clear. The retrieved AODs on this day range up to about 0.3
17 in the vicinity of Osaka, itself. The main difference between the V22 17.6 km AOD map in
18 Fig. 5b and the 4.4 km retrieval map in Fig. 5c is the improvement in coverage due to the
19 relaxation of the χ^2 thresholds in the 4.4 km retrieval. The remaining missing retrievals,
20 indicated in white, are due primarily to the shallow water between Honshu, the main landmass
21 in the upper (northern) portion of the image, and the mountainous island of Shikoku. The
22 MISR Dark Water algorithm does not attempt to perform retrievals in locations identified as
23 “shallow water” due to possible contributions from the underwater surface (e.g., Kahn et al.,
24 2009). Retrievals are also not performed over much of Shikoku due to the complex terrain in
25 the mountains, which violates the assumptions of the 1-D radiative transfer used in the MISR
26 aerosol retrieval algorithm. Although these exclusion conditions apply to both the 17.6 km
27 and 4.4 km algorithms, the higher resolution retrieval typically obtains better coverage by
28 being able to get closer to these exclusion zones. Some of the improved coverage of the 17.6
29 km retrieval, in the lower right portion of the image, for example, is only due to the larger
30 area covered by a single 17.6 km pixel, compared to a single 4.4 km pixel.



1 Figures 6 and 7 show the spatial sampling over South Korea for cases with very high aerosol
2 loads. The white regions in the MISR red band image in Fig. 6a are clouds to the northeast
3 and southwest of the peninsula on 9 May 2012 at the Terra overpass time around 02:20 UTC.
4 The landmass, however, is mainly clear. The V22 17.6 km retrieval does not have coverage
5 over most of the region, and the agreement between the MISR AODs and the AERONET-
6 DRAGON sites (colored circles) is not particularly good. The latter is not surprising given
7 the underestimation at high AOD in the 17.6 km product apparent in Fig. 4a. The 4.4 km
8 aerosol retrieval in Fig. 6b has much better coverage, with the missing locations
9 corresponding well with areas with large amounts of topographic relief. What is particularly
10 striking is the ability of this retrieval to capture the true spatial variability of the aerosol
11 throughout the region, in good agreement with the AERONET-DRAGON observations. In
12 this case, there does not appear to be any high bias due to the presence of urban surfaces,
13 which has been identified as an issue in the MODIS 3 km aerosol product (Munchak et al.,
14 2013). Unfortunately, without ancillary information it is difficult to assess the veracity of the
15 high AODs shown in the vicinity of the clouds in the far right of the image. However, both
16 the 17.6 km and 4.4 km retrievals indicate elevated AODs in this area.

17 The case in Fig. 7 has somewhat lower AODs than the previous case. Figure 7a shows the
18 MISR red band image from 25 May 2012 at around 02:20 UTC. There are orographic clouds
19 along the eastern coast of the Korean peninsula and a solid mass of clouds in the lower right
20 of the image. Again, the V22 17.6 km resolution product shown in Fig. 7b has missing
21 retrievals over much of the landmass. However, there appears to be a northwest to southeast
22 gradient in the AODs, continuing over the water. Figure 7c shows that evidence for this
23 overall gradient is lacking by filling in many of the missing areas. Instead, locations of high
24 AOD appear sporadically in the scene. The highest AODs are found over Seoul, which has
25 the majority of the AERONET-DRAGON sites, a couple of locations to the southeast, and
26 near the edges of the cloud fields. The two locations to the southeast of Seoul correspond to
27 valleys that are likely trapping pollution on this particular date. Again, it is hard to assess the
28 veracity of the high AODs in the lower portion of the image, but at least the two algorithms
29 are consistent with one another.

30



1 **4 Discussion and conclusions**

2 The operational V22 MISR aerosol retrieval algorithm went into production in December
3 2007. Since that time other satellite aerosol retrieval products have undergone significant
4 enhancements, including both the MODIS DT and DB algorithms (Levy et al., 2013; Remer
5 et al., 2013; Sayer et al., 2015). Efforts to improve the MISR aerosol algorithm have focused
6 on the issues noted by Kahn et al. (2010) in their evaluation of the MISR V22 aerosol product
7 against global AERONET observations, as well as topics raised by others (e.g., Kalashnikova
8 et al., 2011; Witek et al., 2013; Shi et al., 2014; and Limbacher and Kahn, 2015). While the
9 air quality community has raised the issue of spatial resolution in terms of using satellite data
10 to study the health impacts of atmospheric aerosols on the appropriate “neighborhood scales,”
11 on the order of one or a few kilometers, the biggest surprise in moving to a higher resolution
12 was the improvement in the retrieved AOD relative to AERONET – an improvement that did
13 not require significant changes to the algorithm itself. This was surprising for two reasons.
14 First, the more or less accepted line of thinking is that aerosols are generally spatially
15 homogeneous at scales of 10’s to 100’s of kilometers, and temporally stationary, in a
16 statistical sense, at time scales of hours to days (e.g., Anderson et al., 2003). Secondly, the
17 MODIS team did not find significant improvement in the performance of their algorithm
18 when they increased the resolution from 10 km to 3 km (Remer et al., 2013). In fact, this
19 change in resolution highlighted some underlying issues in the assumptions going into the DT
20 retrieval (Munchak et al., 2013).

21 Importantly, it would have been difficult to assess the performance of a high-resolution
22 algorithm without appropriate high-resolution observations to evaluate against. A single
23 AERONET site basically returns a “point” in space and time relative to retrievals from a
24 satellite instrument. This has led to the adoption of averaging approaches that require large
25 amounts of paired satellite-AERONET data matched within relatively broad spatial and
26 temporal windows (e.g., Ichoku et al., 2003; Kahn et al., 2010; Petrenko et al., 2012). The
27 deployment of AERONET-DRAGON sites beginning in 2011 has been a game-changer in
28 terms of the ability to truly consider aerosol spatial variability, and the DRAGON
29 deployments at sites around the globe facilitated the analysis presented here.

30 The performance of the operational V22 17.6 km MISR aerosol retrieval relative to the
31 performance of a prototype 4.4 km retrieval was assessed in comparisons with multiple
32 AERONET-DRAGON deployments over a broad range of AODs. It was found that, overall,



1 the 4.4 km retrieval performed significantly better than the 17.6 km retrieval. Part of the
2 reason for this improvement is the ability of the higher-resolution retrieval to capture the true
3 spatial variability of the aerosols, which is also captured by the DRAGON network. Again, a
4 single AERONET site cannot directly represent the spatial variability of aerosols, although
5 this is aliases into the temporal dependence of the AODs reported by the instrument.
6 Averaging the AERONET data over a time window and the satellite data over a spatial
7 window, as is traditionally done in global comparisons, has the effect of minimizing the
8 contributions of true aerosol spatial variability. Another reason for the improvement of the
9 MISR retrieval algorithm when applied at 4.4 km is that the assumptions underlying the
10 aerosol retrieval, particularly over land, are better met at this higher spatial resolution.
11 Ironically, among the most critical of these assumptions is that aerosols are spatially
12 homogeneous on the scale of the retrieval. In other words, aerosol variability itself is one of
13 the issues with the 17.6 km retrieval.

14 The MISR aerosol algorithm team is working toward the release of an updated version of the
15 aerosol retrieval that will have results reported globally at 4.4 km resolution. In addition to
16 this change, other changes and being tested and implemented with regard to cloud screening,
17 per-retrieval uncertainty reporting, and microphysical property retrievals. Critical to the
18 development of this new algorithm are assessments against AERONET-DRAGON
19 deployments for a range of cases represented by those used in this paper.

20

21 **Acknowledgements**

22 This work was performed at the Jet Propulsion Laboratory, California Institute of Technology
23 under a contract with the National Aeronautics and Space Administration. The MISR data
24 used in this work were obtained from the NASA Langley Research Center Atmospheric
25 Science Data Center. We thank the many PI investigators, and particularly the hard work of
26 Brent Holben and his team for establishing and maintaining the AERONET and AERONET-
27 DRAGON sites used in this investigation.

28



1 References

- 2 Anderson, T. L., Charlson, R. J., Winker, D. M., Ogren, J. A., and Holmén, K.: Mesoscale
3 variations of tropospheric aerosols, *J. Atmos. Sci.*, 60, 119–136, 2003.
- 4 Beyersdorf, A. J., Ziemba, L. D., Chen, G., Corr, C. A., Crawford, J. H., Diskin, G. S.,
5 Moore, R. H., Thornhill, K. L., Winstead, E. L., and Anderson, B. E.: The impacts of aerosol
6 loading, composition, and water uptake on aerosol extinction variability in the Baltimore–
7 Washington, D.C. region, *Atmos. Chem. Phys.*, 16, 1003–1015, doi:10.5194/acp-16-1003-
8 2016, 2016.
- 9 Bothwell, G. W., Hansen, E. G., Vargo, R. E., and Miller, K. C.: The Multi-angle Imaging
10 SpectroRadiometer science data system, its products, tools, and performance, *IEEE Trans.*
11 *Geosci. Remote Sens.*, 40, 1467–1476, doi:10.1109/TGRS.2002.801152, 2002.
- 12 Boucher, O., Randall, D., Artaxo, P., Bretherton, C., Feingold, G., Forster, P., Kerminen, V.-
13 M., Kondo, Y., Liao, H., Lohmann, U., Rasch, P., Satheesh, S. K., Sherwood, S., Stevens, B.,
14 and Zhang, X. Y.: Clouds and aerosols in: *Climate Change 2013: The Physical Science Basis.*
15 Contribution of Working Group I to the Fifth Assessment Report of the Intergovernmental
16 Panel on Climate Change, Stocker, T. F., Qin, D., Plattner, G.-K., Tignor, M., Allen, S. K.,
17 Boschung, J., Nauels, A., Xia, Y., Bex, V., and Midgley, P. M. (eds.), 571–657, Cambridge
18 University Press, Cambridge, United Kingdom and New York, NY, USA, 2013.
- 19 Bruegge, C. J., Chrien, N. L., Ando, R. R., Diner, D. J., Abdou, W. A., Helmlinger, M. C.,
20 Pilorz, S. H., and Thome, K. J.: Early validation of the Multi-angle Imaging
21 SpectroRadiometer (MISR) radiometric scale, *IEEE Trans. Geosci. Remote Sens.*, 40, 1477–
22 1492, doi:10.1109/TGRS.2002.801583, 2002.
- 23 Diner, D. J., Beckert, J. C., Reilly, T. H., Bruegge, C. J., Conel, J. E., Kahn, R. A.,
24 Martonchik, J. V., Ackerman, T. P., Davies, R., Gerstl, S. A. W., Gordon, H. R., Muller, J.-P.,
25 Myneni, R. B., Sellers, P. J., Pinty, B., and Verstraete, M. M.: Multi-angle Imaging
26 SpectroRadiometer (MISR) instrument description and experiment overview, *IEEE Trans.*
27 *Geosci. Remote Sens.*, 36, 1072–1087, 1998.
- 28 Diner, D. J., Martonchik, J. V., Kahn, R. A., Pinty, B., Gobron, N., Nelson, D. L., and
29 Holben, B. N.: Using angular and spectral shape similarity constraints to improve MISR
30 aerosol and surface retrievals over land, *Remote Sens. Environ.*, 94, 155–171,
31 doi:10.1016/j.rse.2004.09.009, 2005.



- 1 Eck, T. F., Holben, B. N., Reid, J. S., Arola, A., Ferrare, R. A., Hostetler, C. A., Crumeyrolle,
2 S. N., Berkoff, T. A., Welton, E. J., Lolli, S., Lyapustin, A., Wang, Y., Schafer, J. S., Giles,
3 D. M., Anderson, B. E., Thornhill, K. L., Minnis, P., Pickering, K. E., Loughner, C. P.,
4 Smirnov, A., and Sinyuk, A.: Observations of rapid aerosol optical depth enhancements in the
5 vicinity of polluted cumulus clouds, *Atmos. Chem. Phys.*, 14, 11633–11656, doi:10.5194/acp-
6 14-11633-2014, 2014.
- 7 Holben, B. N., Eck, T. F., Slutsker, I., Tanré, D., Buis, J. P., Setzer, A., Vermote, E., Reagan,
8 J. A., Kaufman, Y. J., Nakajima, T., Lavenue, F., Jankowiak, I., and Smirnov, A.: AERONET
9 – A federated instrument network and data archive for aerosol characterization, *Remote Sens.*
10 *Environ.*, 66, 1–16, 1998.
- 11 Ichoku, C., Chu, D., A., Mattoo, S., Kaufman, Y. J., Remer, L. A., Tanré, D., Slutsker, I., and
12 Holben, B. N.: A spatio-temporal approach for global validation and analysis of MODIS
13 aerosol products, *Geophys. Res. Lett.*, 29, 1616, doi:10.1029/2001GL013206, 2002.
- 14 Kahn, R. A., Gaitley, B. J., Garay, M. J., Diner, D. J., Eck, T. F., Smirnov, A., and Holben, B.
15 N.: Multiangle Imaging Spectroradiometer global aerosol product assessment by comparison
16 with the Aerosol Robotic Network, *J. Geophys. Res.*, 115, D23209,
17 doi:10.1029/2010JD014601, 2010.
- 18 Kahn, R. A., Nelson, D. L., Garay, M. J., Levy, R. C., Bull, M. A., Diner, D. J., Martonchik,
19 J. V., Paradise, S. R., Hansen, E. G., and Remer, L. A.: MISR aerosol product attributes and
20 statistical comparisons with MODIS, *IEEE Trans. Geosci. Remote Sens.*, 47, 4095–4114,
21 doi:10.1109/TGRS.2009.2023115, 2009.
- 22 Kalashnikova, O. V., Garay, M. J., Martonchik, J. V., and Diner, D. J.: MISR Dark Water
23 aerosol retrievals: operational algorithm sensitivity to particle non-sphericity, *Atmos. Meas.*
24 *Tech.*, 6, 2131–2154, doi:10.5194/amt-6-2131-2013, 2013.
- 25 Levy, R. C., Mattoo, S., Munchak, L. A., Remer, L. A., Sayer, A. M., Patadia, F., and Hsu, N.
26 C.: The Collection 6 MODIS aerosol products over land and ocean, *Atmos. Meas. Tech.*, 6,
27 2989–3034, doi:10.5194/amt-6-2989-2013, 2013.
- 28 Limbacher, J. A., and Kahn, R. A.: MISR empirical stray light corrections in high-contrast
29 scenes, *Atmos. Meas. Tech.*, 8, 2927–2943, 2015.
- 30 Martin, R. V.: Satellite remote sensing for air quality, *Atmos. Environ.*, 42, 7823 – 7843,
31 doi:10.1016/j.atmosenv.2008.07.018, 2008.



- 1 Martonchik, J. V., Kahn, R. A., and Diner, D. J.: Retrieval of aerosol properties over land
2 using MISR observations, in Satellite Aerosol Remote Sensing of Land, Kokhanovsky, A.,
3 A., and de Leeuw, G. (eds.), Springer, Berlin, 267–293, doi:10.1007/978-3-540-69397-0_9,
4 2009.
- 5 Munchak, L. A., Levy, R. C., Mattoo, S., Remer, L. A., Holben, B. N., Schafer, J. S.,
6 Hostetler, C. A., and Ferrare, R. A.: MODIS 3 km aerosol product: applications over land in
7 an urban/suburban region, Atmos. Meas. Tech., 6, 1747–1759, doi:10.5194/amt-6-1747-2013,
8 2013.
- 9 Petrenko, M., Ichoku, C., and Leptoukh, G.: Multi-sensor Aerosol Products Sampling System
10 (MAPSS), Atmos. Meas. Tech., 5, 913–926, doi:10.5194/amt-5-913-2012, 2012.
- 11 Remer, L. A., Mattoo, S., Levy, R. C., and Munchak, L. A.: MODIS 3 km aerosol product:
12 algorithm and global perspective, Atmos. Meas. Tech., 6, 1829–1844, doi:10.5194/amt-6-
13 1829-2013, 2013.
- 14 Sano, I., Mukai, S., Nakata, M., and Holben, B. N.: Regional and local variations in
15 atmospheric aerosols using ground-based sun photometry during DRAGON in 2012, Atmos.
16 Chem. Phys. Discuss., doi:10.5194/acp-2016-381, 2016.
- 17 Sayer, A. M., Hsu, N. C., Bettenhausen, C., and Jeong, M.-J.: Validation and uncertainty
18 estimates for MODIS Collection 6 “Deep Blue” aerosol data, J. Geophys. Res. Atmos., 118,
19 7864–7873, doi:10.1002/jgrd.50600, 2013.
- 20 Sayer, A. M., Hsu, N. C., Bettenhausen, C., Jeong, M.-J., and Meister, G.: Effect of MODIS
21 Terra radiometric calibration improvements on Collection 6 Deep Blue aerosol products:
22 Validation and Terra/Aqua consistency, J. Geophys. Res. Atmos., 120, 12,157–12,174,
23 doi:10.1002/2015JD023878, 2015.
- 24 Seo, S., Kim, J., Lee, H., Jeong, U., Kim, W., Holben, B. N., Kim, S.-W., Song, C. H., Lim,
25 and Lim, J. H.: Estimation of PM₁₀ concentrations over Seoul using multiple empirical
26 models with AERONET and MODIS data collected during the DRAGON-Asia campaign,
27 Atmos. Chem. Phys., 15, 319–334, doi:10.5194/acp-15-319-2015, 2015.
- 28 Shi, Y., Zhang, J., Reid, J. S., Hyer, E. J., Eck, T. F., Holben, B. N., and Kahn, R. A.: A
29 critical examination of spatial biases between MODIS and MISR aerosol products –
30 application for potential AERONET deployment, Atmos. Meas. Tech., 4, 2823–2836,
31 doi:10.5194/amt-4-2823-2011, 2011.



- 1 van Donkelaar, A., Martin, R. V., Brauer, M., and Boys, B. L.: Use of satellite observations
- 2 for long-term exposure assessment of global concentrations of fine particulate matter,
- 3 Environ. Health Persp., 123, 135–143, doi:10.1289/ehp.1408646, 2015.
- 4 van Donkelaar, A., Martin, R. V., Brauer, M., Hsu, N. C., Kahn, R. A., Levy, R. C.,
- 5 Lyapustin, A., Sayer, A. M., and Winker, D. M.: Global estimates of fine particulate matter
- 6 using a combined geophysical-statistical method with information from satellites, models, and
- 7 monitors, Environ. Sci. Technol., 50, 3762–3772, doi:10.1021/acs.est.5b05833, 2016.
- 8 Witek, M. L., Garay, M. J., Diner, D. J., and Smirnov, A.: Aerosol optical depths over oceans:
- 9 A view from MISR retrievals and collocated MAN and AERONET in situ observations, J.
- 10 Geophys. Res. Atmos., 118, 1–14, doi:10.1002/2013JD020393, 2013.

11



1 Table 1. Spatial statistics of AERONET-DRAGON deployments.

DRAGON Campaign	Sites	Pairs	Separation < 17.6 km	Separation < 8.8 km	Separation < 4.4 km	Mean Separation (km)	Median Separation (km)
USA 2011 (Washington D.C., Baltimore)	46	1035	105	21	2	51.4	42.6
Asia 2012 (Japan, South Korea)	53	1378	54	22	11	525.9	543.0
SE Asia 2012 (7-SEAS)	46	1035	31	8	3	1927.0	1877.5
USA 2012-2013 (San Joaquin Valley)	28	378	7	3	1	245.7	204.8
Germany 2013 (HOPE)	15	105	3	3	1	359.2	397.4
USA 2013 (Houston)	19	171	6	2	1	103.3	66.1
USA 2013 (SEAC ⁴ RS)	54	1431	9	5	3	993.6	989.0
USA 2014 (Colorado)	15	105	6	1	0	87.1	53.1

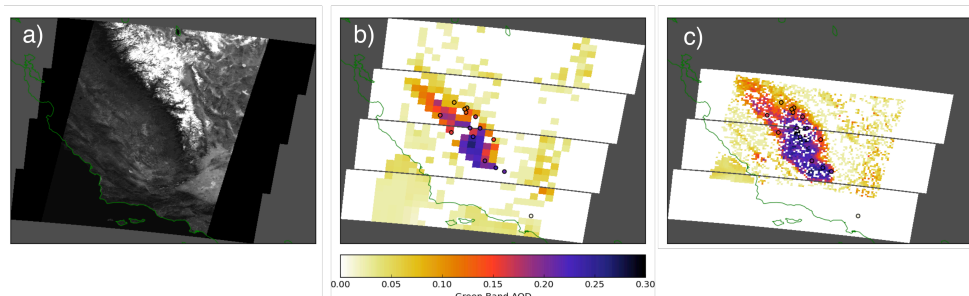
2



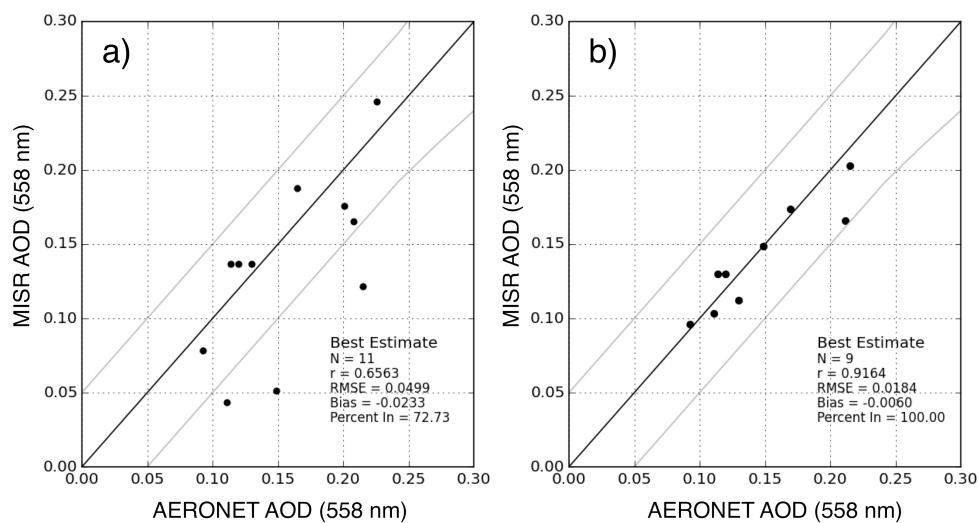
1 Table 2. MISR cases for AERONET-DRAGON comparison.

Orbit	Date/Time	Campaign	SOM Path	MISR Blocks	Notes
60934	2011-06-02 16:05 UTC	Washington, Baltimore	16	58-60	Low AOD, Clear
61633	2011-07-20 16:05 UTC	Washington, Baltimore	16	58-60	Moderate AOD, Scattered Clouds
61662	2011-07-22 15:55 UTC	Washington, Baltimore	14	58-60	Moderate AOD, Scattered Clouds
65440	2012-04-07 02:20 UTC	Asia-Seoul	115	60-62	Low AOD, Clear
65731	2012-04-27 01:55 UTC	Asia-Osaka	111	62-64	Low AOD, Clear
65775	2012-04-30 02:25 UTC	Asia-Seoul	116	60-62	Moderate AOD, Clear
65906	2012-05-09 02:20 UTC	Asia-Seoul	115	60-62	High AOD, Hazy
66139	2012-05-25 02:20 UTC	Asia-Seoul	115	60-62	High AOD, Hazy
69644	2013-01-20 18:50 UTC	San Joaquin Valley	42	60-63	Low AOD, Clear
69877	2013-02-05 18:50 UTC	San Joaquin Valley	42	60-63	Moderate AOD, Few Clouds

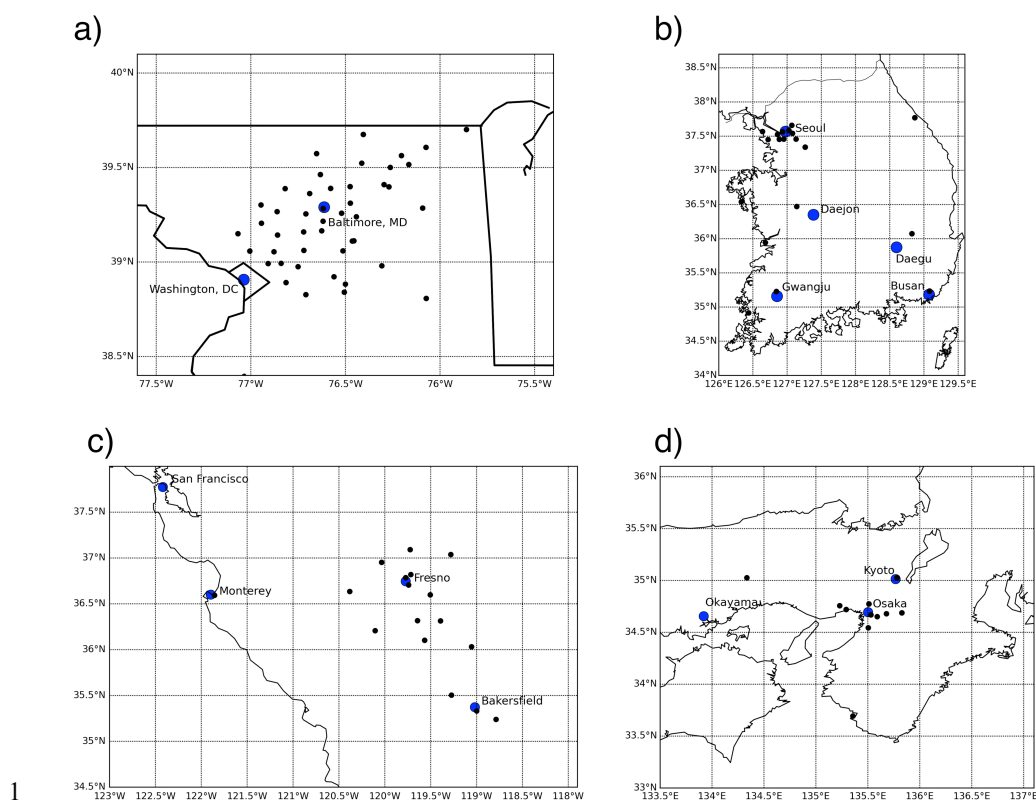
2



1
 2 Figure 1. (a) MISR red band image of the San Joaquin Valley in California on 20 January
 3 2013 at around 18:50 UTC; (b) MISR V22 17.6 km aerosol optical depth (AOD); (c) MISR
 4 4.4 km AOD retrieved using a modified version of the V22 aerosol retrieval algorithm with
 5 275 m local mode data as input.
 6

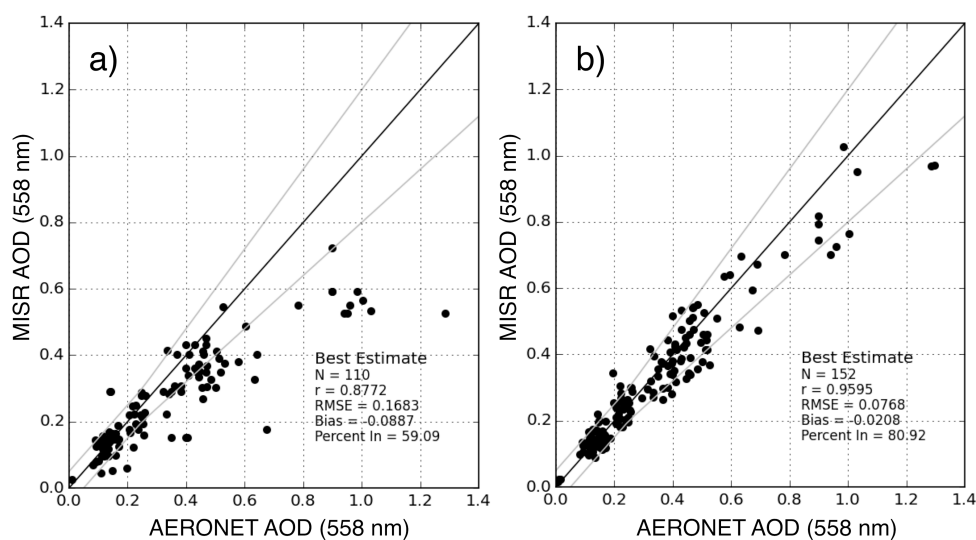


1
 2 Figure 2. (a) Regression of MISR V22 17.6 km resolution AODs against AERONET
 3 interpolated to the MISR wavelength. (b) Regression of the 4.4 km resolution AODs against
 4 AERONET.
 5
 6

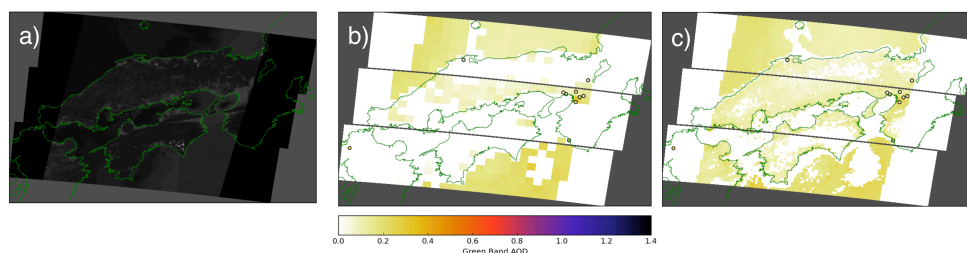


1
 2 Figure 3. (a) Locations of the 45 sites deployed as part of the AERONET-DRAGON
 3 campaign in Washington, D.C./Baltimore metropolitan area; (b) Locations of the 25 sites
 4 deployed in South Korea during DRAGON-Asia 2012; (c) Locations of the 18 sites deployed
 5 in the San Joaquin Valley in California in late 2012 and early 2013; (d) Location of the 14
 6 sites deployed in Japan during DRAGON-Asia 2012.

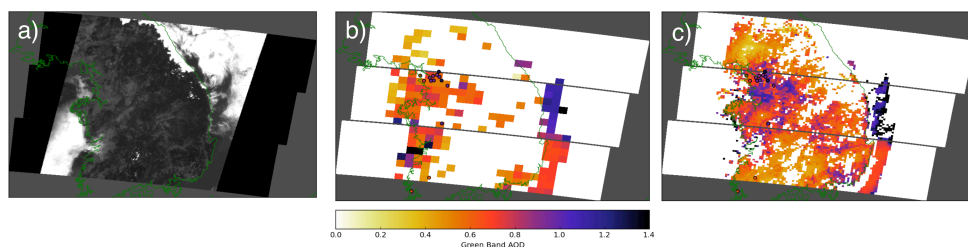
7



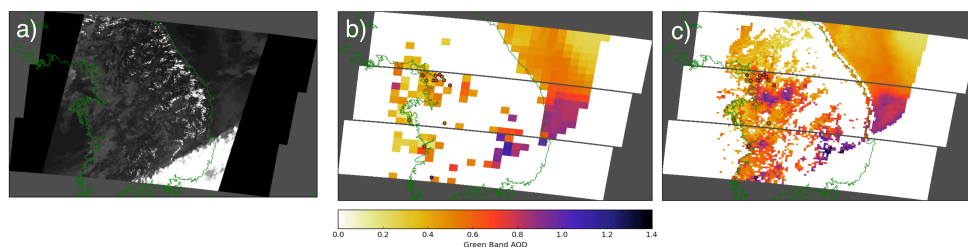
1
 2 Figure 4. (a) Regression of MISR V22 17.6 km resolution AODs against AERONET
 3 interpolated to the MISR wavelength. (b) Regression of the 4.4 km resolution AODs against
 4 AERONET.
 5



1
 2 Figure 5. (a) MISR red band image of the Osaka, Japan on 27 April 2012 at around 01:55
 3 UTC; (b) MISR V22 17.6 km aerosol optical depth (AOD); (c) MISR 4.4 km AOD retrieved
 4 using a prototype algorithm that takes the 1.1 km global data as input.
 5



1
2 Figure 6. (a) MISR red band image of the Korea on 09 May 2012 at around 02:20 UTC; (b)
3 MISR V22 17.6 km aerosol optical depth (AOD); (c) MISR 4.4 km AOD retrieved using the
4 prototype algorithm.
5



1
2 Figure 7. (a) MISR red band image of the Korea on 25 May 2012 at around 02:20 UTC; (b)
3 MISR V22 17.6 km aerosol optical depth (AOD); (c) MISR 4.4 km AOD retrieved using the
4 prototype algorithm.